

Size-selective contrasting of cracks on a metal surface by gold nanoparticles

Mikhail S. Kotelev, Dmitry S. Kopitsyn, Ivan A. Tiunov,
Vladimir A. Vinokurov and Andrei A. Novikov*

Center for Nanodiagnostics, Department of Physical and Colloid Chemistry, I. M. Gubkin Russian State University of Oil and Gas, 119991 Moscow, Russian Federation. E-mail: novikov.a@gubkin.ru

DOI: 10.1016/j.mencom.2015.09.013

The size-selective contrasting of nanosized surface defects by photoluminescent metal nanoparticles is proposed.

Pipeline corrosion is the major threat to the oil and gas transport infrastructure in harsh climate regions such as Ural and Siberia in Russia. Various nondestructive testing (NDT) methods are available for the monitoring of corrosion in oil and gas equipment. Recent developments in optical NDT methods are focused on the detection of defects close to the diffraction limit by size: the detection of subpixel-sized defects by infrared thermography,¹ the monitoring of pitting corrosion by the measurement of pit depth by confocal microscopy² and the confocal Raman mapping of a metal surface.³ Among the oldest, simplest and cheapest optical NDT methods are dye penetrant methods.⁴ Unfortunately, dye penetrant methods are not applicable to rough surfaces, their contrasting ability is low, and the microcrack size estimation is unavailable. In order to provide size-selective contrast, the penetrant nanoparticles should be either photoluminescent or grafted with fluorescent dyes. Photoluminescent metal nanoparticles are superior to fluorescent dyes in photostability⁵ and to semiconductor quantum dots in biocompatibility.⁶ Earlier,⁷ surface defects on pipeline steel samples contrasted by core-shell copper-silica nanoparticles were detected.

The aim of this work was to develop an NDT procedure providing the size-selective detection of mapped surface defects contrasted by photoluminescent metal nanoparticles. The method is based on the detection of nanoparticle photoluminescence and second harmonics generation⁸ with excitation by a femtosecond near-infrared laser.

Gold nanoparticles stabilized by citrate were synthesized via a modified technique⁹ in a water-jacketed four-necked flask equipped with a thermometer, a reflux condenser and a dropping funnel. The fourth neck was used for sampling. All the glassware was soaked in *aqua regia* prepared daily and rinsed with deionized water[†] afterwards. The temperature in the flask was 90.0 ± 0.1 °C during the synthesis.[‡] Gold nanoparticles stabilized by gum arabic were synthesized¹⁰ in the same apparatus at room temperature. Nanoparticles were characterized by transmission electron microscopy (TEM),[§] using the ImageJ software¹¹ for the measurement of diameters of at least 150 individual particles. The characteristics estimated by the image analysis are reported in the (mean \pm sample standard deviation) format. Model nanocracks were etched on the surface of X70 pipeline steel specimens by a focused ion beam[¶] and then imaged on the same apparatus in the scanning electron microscope (SEM) mode. The nano-

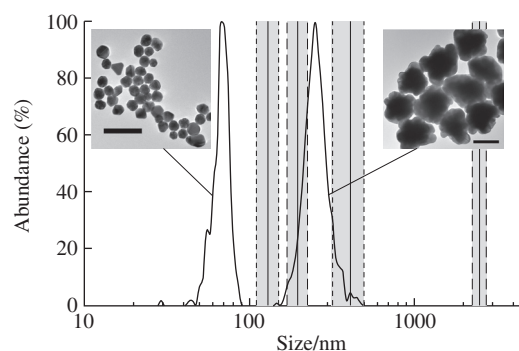


Figure 1 Size distribution of the gold nanoparticles stabilized by citrate (66 ± 8 nm) and gum arabic (252 ± 45 nm), and size distribution of nanocracks (130 ± 20 , 196 ± 27 , 406 ± 89 and 2480 ± 240 nm). Insets: TEM micrographs of gold nanoparticles (scale bar, 200 nm).

cracks were etched in ensembles for their recognition in optical micrographs, with the repeated pattern of the nanocracks 2500, 400, 200 and 130 nm wide. Figure 1 shows the size distribution of nanoparticles and the widths of the model nanocracks.

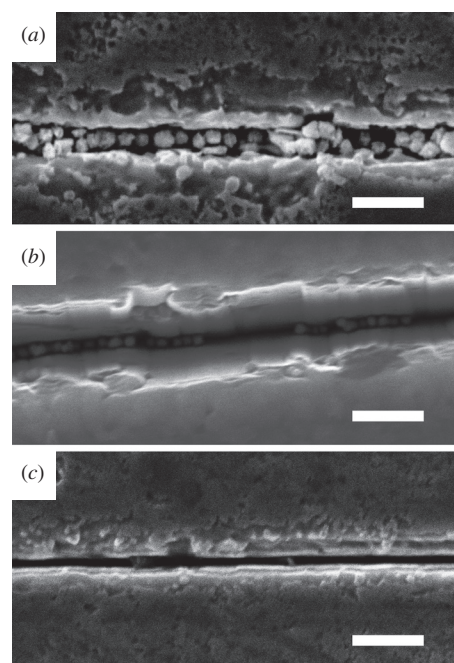


Figure 2 SEM micrographs of the model nanocracks (a) 406 ± 89 , (b) 196 ± 27 and (c) 130 ± 20 nm wide contrasted by the gold nanoparticles stabilized by gum arabic. Scale bar, 1 μ m.

[†] 18 M Ω cm, Simplicity UV, Millipore, USA.

[‡] FBH-712, Fischerbrand, Germany.

[§] JEM-2100, Jeol, Japan.

[¶] JIB-4501, Jeol, Japan.



Figure 3 Micrographs of the nanocrack ensemble: (a) optical microscopy, (b) map of the photoluminescence of gold nanoparticles stabilized by gum arabic and (c) map of the photoluminescence of gold nanoparticles stabilized by citrate. Scale bar, 50 μm .

The model nanocracks were contrasted at first with the gold nanoparticles stabilized by gum arabic, imaged, and then contrasted once again with the gold nanoparticles stabilized by citrate. SEM micrographs of the contrasted nanocracks are shown in Figure 2.

The gold nanoparticles with a diameter of 252 ± 45 nm contrasted the nanocracks of 406 ± 89 nm wide and the nanocracks of 196 ± 27 nm wide but with lower loading, and leave the nanocracks of 130 ± 20 nm wide uncontrasted. Thus, the application of gold nanoparticles to the pipeline steel specimens could be used as the size-selective contrasting of surface defects.

The specimens were observed under an inverted microscope,^{††} and the distribution of nanoparticles on the specimens was assessed by photoluminescence microscopy.¹² The nanoparticles were excited with a 1048 nm femtosecond laser at a power density of 1.16×10^9 W m^{-2} , and their photoluminescence intensity was measured by a photomultiplier. Using a motorized x - y stage, we scanned the specimens and recorded the map of nanoparticle photoluminescence (Figure 3).

Figure 3 shows that all the used nanoparticles sharply contrasted the widest model crack (the most left, 2480 ± 240 nm wide). However, the contrast of the nanocracks with a width close to the size of the nanoparticles [Figure 3(b), nanoparticles diameter is 252 ± 45 nm; the second and third nanocracks are 406 ± 89 nm and 196 ± 27 nm wide, respectively] was significantly lower. The narrowest nanocrack (130 ± 20 nm wide) was not contrasted by the nanoparticles. All the nanocracks were contrasted by sufficiently small (66 ± 8 nm) gold nanoparticles [Figure 3(c)].

In contrast to previously published data,⁷ we found for the first time the size-selective contrasting of surface defects by the consequent application of nanoparticles larger and smaller than the defect. The resolution of the method can be improved using uniform nanoparticles. We used the citrate-stabilized gold nanoparticles with a diameter of 66 ± 8 nm and a polydispersity index (PDI) of 0.117, and the gum arabic-stabilized gold nanoparticles with a diameter of 252 ± 45 nm and a PDI of 0.179. However, published data suggest that these nanoparticles could be obtained with PDIs of 0.052⁹ and 0.088 for the citrate- and gum arabic-stabilized ones. The sensitivity of the method depends on the particle size. The photoluminescence of silver nanoparticles has a maximum for a particle size of ~ 30 nm with xenon lamp excitation.¹³ With femtosecond laser excitation, the largest photoluminescence is provided by gold nanoparticles with a particle size of 55–80 nm and silver nanoparticles with a particle size

of about 50 nm.¹⁴ Thus, the sensitivity of the method is maximal for defects larger than 50 nm. Note that the apparatus used for the photoluminescence mapping of samples can be essentially simplified in order to achieve the capability of routine examination of metal surfaces contrasted by nanoparticles. Furthermore, femtosecond lasers are becoming more popular in ophthalmology, and their large-scale production will lower the cost of laser significantly.

As we expected, the gold nanoparticles with a narrow size distribution can be employed as size-selective optical markers for the detection of surface defects. The model nanocracks barely visible on optical micrographs are sharply contrasted on photoluminescence micrographs, and surface defects can be differentiated by width using nanoparticles larger and smaller than the width of defects. The reported method of the size-selective contrasting of surface defects can be applied to the nondestructive testing of surface corrosion defects at the earlier stages of growth.

This work was supported by the Ministry of Education and Science of the Russian Federation (project no. 1256). We are grateful to M. Gorbachevskii (I. M. Gubkin Russian State University of Oil and Gas, Moscow) for his assistance in the synthesis of nanoparticles and to A. Pecheny (Yandex, Moscow) for the preparation of the manuscript and to anonymous reviewers for valuable comments.

References

- 1 C. J. Earls, *Mech. Systems Signal Proc.*, 2012, **30**, 146.
- 2 M. Jasiczek, J. Kaczorowski, E. Kosieniak and M. Innocenti, *J. Failure Anal. Prevent.*, 2012, **12**, 305.
- 3 G. Gouadec, L. Bellot-Gurlet, D. Baron and P. Colomban, in *Raman Imaging*, ed. A. Zoubir, Springer, Berlin–Heidelberg, 2012, pp. 85–118.
- 4 F. Hernandez-Valle, A. R. Clough and R. S. Edwards, *Corros. Sci.*, 2014, **78**, 335.
- 5 R. A. Farrer, F. L. Butterfield, V. W. Chen and J. T. Fourkas, *Nano Lett.*, 2005, **5**, 1139.
- 6 Y. Song, D. Feng, W. Shi, X. Li and H. Ma, *Talanta*, 2013, **116**, 237.
- 7 M. E. Bardin, A. V. Savin, E. V. Ivanov, P. A. Gushchin, V. A. Vinokurov, A. V. Muradov and L. T. Perelman, *Korroziya: Materialy, Zashchita*, 2014, **5**, 13 (in Russian).
- 8 H.-D. Deng, G.-C. Li, Q.-F. Dai, M. Ouyang, S. Lan, V. A. Trofimov and T. M. Lysak, *Nanotechnology*, 2013, **24**, 075201.
- 9 N. G. Bastus, J. Comenge and V. Puentes, *Langmuir*, 2011, **27**, 11098.
- 10 H. Wang and N. J. Halas, *Adv. Mater.*, 2008, **20**, 820.
- 11 C. A. Schneider, W. S. Rasband and K. W. Eliceiri, *Nat. Methods*, 2012, **9**, 671.
- 12 D. S. Sitnikov, A. A. Yurkevich, M. S. Kotelev, M. Ziangiurova, O. V. Chefonov, I. V. Ilina, V. A. Vinokurov, A. V. Muradov, I. Itzkan, M. B. Agranat and L. T. Perelman, *Laser Phys. Lett.*, 2014, **11**, 075902.
- 13 O. A. Yeshchenko, I. M. Dmitruk, A. A. Alexeenko, M. Yu. Losytskyy, A. V. Kotko and A. O. Pinchuk, *Phys. Rev. B*, 2009, **79**, 235438.
- 14 F. Han, Z. Guan, T. S. Tan and Q.-H. Xu, *ACS Appl. Mater. Interfaces*, 2012, **4**, 4746.

^{††} IX-71, Olympus, Japan.

Received: 15th December 2014; Com. 14/4529